A Fast and Reliable Method for Computer Analysis of Microwave Mixers

BERND SCHÜPPERT

Abstract—**In this paper, a numerical method is presented for analyzing microwave mixers. Particular consideration is given to the solution of the nonlinear pumping problem of real Schottky-barrier diodes. The new technique has a significantly improved convergence rate, which is demonstrated by means of direct comparisons with other methods. A convergence test procedure is proposed and applied which uses randomly generated harmonic impedances.**

The proposed numerical technique for solving the nonlinear and linear problem is extended to the analysis of balanced mixers. Fabricated planar balanced mixers are analyzed, both theoretically and experimentally, in a separate paper.

I. Introduction

MANY AUTHORS have dealt with the problem of analyzing a mixer's behavior since Thorrey and Whitmer [1] presented their fundamental mixer analysis. As faster computers are now available, more sophisticated mixer models have been established.

Even though the application of MESFET preamplifiers makes the question of the mixer sensitivity less important in the frequency range up to about 10 GHz, efficient and reliable design and analysis techniques for millimeter-wave mixers are still required [2], [3]. Hence, this paper is intended to contribute to this field by means of presenting an efficient and reliable numerical technique for solving the nonlinear mixer problem.

Up to now, single-ended mixers have been preferably considered, whereas only two papers have dealt with balanced mixers [4], [5]. Due to the fact that the local oscillator (LO) and signal frequency power levels are of different orders of magnitude, the analysis of a mixer can be split into a nonlinear analysis, taking the LO into account, and a linear analysis, which describes the frequency conversion between signal and intermediate frequency by means of a linearized conversion matrix.

The dominant problem of a mixer analysis is the determination of the coefficients of the conversion matrix by means of a nonlinear analysis. Different numerical techniques have been published [6]–[11] with convergence rates which differ significantly. In this paper, a modification of reference [7] will be presented in detail, which has been described briefly in [11]. The basic idea of this modification is to use the effective harmonic impedances of the diode in determining the successive corrections as the solution converges. Using the particular set of harmonic impedances and diode data as considered in [6], [8], and [12], the convergence rate is increased by more than a factor of ten.

The accuracy of predicting a mixer's behavior by the proposed numerical technique will be demonstrated by a comparison of theoretical and experimental results which will be given in a separate paper [13]. Even though the noise behavior of a mixer is its most important specification, only the conversion loss will be considered here. However, it can be expected that a numerical technique which yields an accurate prediction of a mixer's conversion loss may simply be extended to a noise characterization as given in [4].

Manuscript received April 1, 1985; revised August 6, 1985

The author is with the Technische Universität Berlin, Institut für Hochfrequenztechnik, Einsteinufer 25, D-1000 Berlin 10, West Germany.

IEEE Log Number 8405928.

II. Nonlinear Analysis

A. Formulating the Problem

Nonlinear devices such as diodes are readily characterized in the time domain by their instantaneous values. Normally, the embedding network is best described in the frequency domain by means of harmonic impedances. At higher frequencies when using distributed elements, it is impossible to give a lumped-element representation of the embedding network. Thus, the analysis has to be split-up into the time and frequency domains as shown in Fig. 1.

The time-domain description is given by

$$i_D = I_s\left(e^{u_D/\eta U_T} - 1\right) + C_j(u_D)\frac{du_D}{dt} \tag{1}$$

where

$$C_j(u_D) = \frac{C_{j0}}{\left(1 - \dfrac{u_D}{\psi}\right)^{\gamma}} \tag{2}$$

$$G_j(u_D) = \frac{I_s}{\eta \cdot U_T} e^{u_D/\eta U_T} \tag{3}$$

and where

- C_{j0} barrier capacitance at $U_D = 0$ V,
- ψ barrier potential,
- γ exponent,
- η ideality factor,
- U_T $(k \cdot T)/e$,
- I_S saturation current.

The frequency-domain requirements due to the embedding

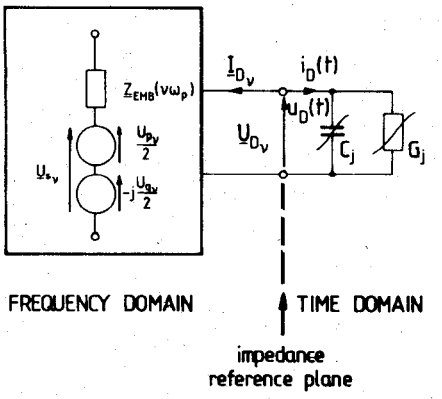

Fig. 1. Time- and frequency-domain description of a mixer consisting of a diode and an embedding network.

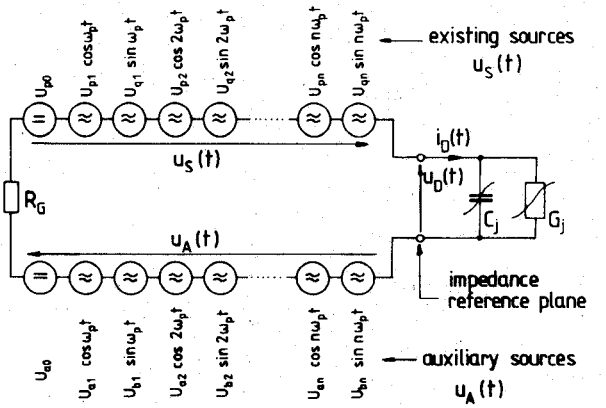

Fig. 2. Time-domain formulation of the nonlinear problem.

network are

$$\underline{I}_{D_\nu} = \frac{\underline{U}_{S\nu} - \underline{U}_{D\nu}}{\underline{Z}_{\mathrm{EMB}}(\nu\omega_p)} \tag{4}$$

where

$$\underline{U}_{S\nu} = \frac{1}{T}\int_0^T u_S(t)\, e^{-j\nu\omega_p t}\, dt = \frac{1}{2}\left(U_{p\nu} - jU_{q\nu}\right) \tag{5}$$

$$\underline{U}_{D\nu} = \frac{1}{T}\int_0^T u_D(t)\, e^{-j\nu\omega_p t}\, dt \tag{6}$$

are the Fourier-transforms of the existing sources $u_S(t)$ and the voltage at the reference plane $u_D(t)$, respectively.

The problem to be solved in the time domain is sketched in Fig. 2 with a mathematical description given by the differential equation

$$\frac{du_D(t)}{dt} = \frac{\left(1 - \dfrac{u_D(t)}{\psi}\right)^{\gamma}}{C_{j0}} \cdot \left\{ \left(u_S(t) + u_A(t) - u_D(t)\right) \Big/ R_{\mathrm{GEN}} - I_s\left(e^{u_D(t)/\eta U_T} - 1\right) \right\} \tag{7}$$

where $u_S(t)$ represents the existing sources

$$u_S(t) = U_{p0} + \sum_{\nu=1}^{n} \left(U_{p\nu}\cos\nu\omega_p t + U_{q\nu}\sin\nu\omega_p t\right). \tag{8}$$

In general, we have only two dominant existing sources

$$U_{p0} = U_{\mathrm{bias}}, \qquad \text{bias}$$

$$U_{p1}\cos\omega_p t = U_p, \qquad \text{first LO harmonic}$$

but the formulation of a set of existing harmonic sources allows to take higher LO harmonics into account, i.e., if the LO source voltage waveform is nonsinusoidal.

It should be noted that the impedance R_G is an arbitrary time-domain representation of the LO source impedance and is not identical with Z_{EMB}. The existence of R_G provides a limitation of the current flow at all LO harmonics.

The quantity $u_A(t)$ represents auxiliary sources as introduced by Gwarek [7], which are intended to balance the harmonic impedances at the impedance reference plane in such a way that the circuit to the left of the reference plane (Fig. 2) is indistinguishable from the embedding circuit on the left of the reference plane in Fig. 1:

$$u_A(t) = U_{a0} + \sum_{\nu=1}^{\eta} \left(U_{a\nu}\cos\nu\omega_p t + U_{b\nu}\sin\nu\omega_p t\right). \tag{9}$$

Establishing auxiliary sources even for average and the first harmonic allows R_{GEN} to be arbitrary, i.e., purely resistive in order to simplify the mathematical description.

It is now necessary to determine the auxiliary sources satisfying the impedance conditions of (4) in the frequency domain. Due to the fact, that the nonlinear element acts as an harmonic generator, no closed-form solution of this problem is available, and the steady state of this network has to be calculated iteratively over a number of LO periods. Following Gwarek and allowing R_{GEN} to become a complex quantity, the change of the auxiliary source of the νth harmonic to be used in the k-th iteration is given by

$$\Delta\underline{U}_\nu^{(k)} = \underline{I}_{D\nu}^{(k-1)} \cdot \underline{Z}_{\mathrm{EMB}}(\nu\omega_p) - \underline{U}_{D\nu}^{(k-1)} + \underline{U}_{S\nu} \tag{10}$$

if the current remains constant, and by

$$\Delta\underline{U}_\nu^{(k)} = \frac{\underline{Z}_{\mathrm{GEN}}(\nu\cdot\omega_p)}{\underline{Z}_{\mathrm{EMB}}(\nu\omega_p)} \left\{ \underline{I}_{D\nu}^{(k-1)} \cdot \underline{Z}_{\mathrm{EMB}}(\nu\omega_p) - \underline{U}_{D\nu}^{(k-1)} + \underline{U}_{S\nu} \right\} \tag{11}$$

if the voltage remains constant.

These conditions imply that the diode acts either as an ideal current generator (10) or as an ideal voltage generator (11) at the νth harmonic. It is obvious that in practice this is not the case, leading to convergence problems for many practical harmonic impedances.

The auxiliary sources for the kth iteration period are given by

$$\underline{U}_{a\nu} = 2\sum_{L=1}^{k} \mathrm{Re}\left\{\Delta\underline{U}_\nu^{(L)}\right\} \tag{12}$$

$$\underline{U}_{b\nu} = -2\sum_{L=1}^{k} \mathrm{Im}\left\{\Delta\underline{U}_\nu^{(L)}\right\}. \tag{13}$$

B. Modification of the Nonlinear Analysis

The idea of the modification is to take into account the harmonic generation of the diode in each LO period and to classify it by its source impedance at each harmonic.

First, (10) and (11) should be rewritten in the following form, where we introduce subscript i for $i = \text{const}$ and subscript u for $u = \text{const}$:

$$\Delta\underline{U}_{i\nu}^{(k)} = \underline{I}_{D\nu}^{(k-1)} \cdot \underline{Z}_{\text{EMB}}(\nu\omega_p) - \underline{U}_{D\nu}^{(k-1)} + \underline{U}_{S\nu}$$

$$\Delta\underline{U}_{u\nu}^{(k)} = \frac{\underline{Z}_{\text{GEN}}(\nu\omega_p)}{\underline{Z}_{\text{EMB}}(\nu\omega_p)} \cdot \Delta\underline{U}_{i\nu}^{(k)}. \tag{15}$$

Knowing the source impedance of the harmonic generator, $Z_D(\nu\omega_p)$ to be defined below, the change of the auxiliary source at the νth harmonic may be written in terms of a change due to $i = \text{const}$ and a change due to $u = \text{const}$, leading to

$$\Delta\underline{U}_{\nu}^{(k)} = \Delta\underline{U}_{i\nu}^{(k)} \left\{ \underline{F}_1(\nu\omega_p) + \frac{\underline{Z}_{\text{GEN}}(\nu\omega_p)}{\underline{Z}_{\text{EMB}}(\nu\omega_p)} \cdot \underline{F}_2(\nu\omega_p) \right\}. \tag{16}$$

For specific values of Z_D, the functions F_1 and F_2 must satisfy the following conditions:

$$\underline{F}_1(\nu\omega_p) \begin{cases} \to 0 \\ = \dfrac{1}{2} \\ \to 1 \end{cases} \quad \text{for} \left| \frac{\underline{Z}_D(\nu\omega_p)}{\underline{Z}_{\text{EMB}}(\nu\omega_p)} \right| \begin{cases} \ll 1 & (u = \text{const.}) \\ = 1 & \\ \gg 1 & (i = \text{const.}) \end{cases} \tag{17}$$

$$\underline{F}_2(\nu\omega_p) \begin{cases} \to 0 \\ = \dfrac{1}{2} \\ \to 1 \end{cases} \quad \text{for} \left| \frac{\underline{Z}_D(\nu\omega_p)}{\underline{Z}_{\text{EMB}}(\nu\omega_p)} \right| \begin{cases} \ll 1 & (i = \text{const.}) \\ = 1 & \\ \ll 1 & (u = \text{const.}) \end{cases} \tag{18}$$

It can be easily verified that these conditions are fulfilled by choosing

$$\underline{F}_1(\nu\omega_p) = \frac{\underline{Z}_D(\nu\omega_p)}{\underline{Z}_D(\nu\omega_p) + \underline{Z}_{\text{EMB}}(\nu\omega_p)} \tag{19}$$

$$\underline{F}_2(\nu\omega_p) = \frac{\underline{Z}_{\text{EMB}}(\nu\omega_p)}{\underline{Z}_D(\nu\omega_p) + \underline{Z}_{\text{EMB}}(\nu\omega_p)} \tag{20}$$

so that (16) can be written as

$$\Delta\underline{U}_{\nu}^{(k)} = \frac{\underline{Z}_D^{(k)}(\nu\omega_p) + \underline{Z}_{\text{GEN}}(\nu\omega_p)}{\underline{Z}_D^{(k)}(\nu\omega_p) + \underline{Z}_{\text{EMB}}(\nu\omega_p)} \cdot \left\{ \underline{I}_{D\nu}^{(k-1)} \underline{Z}_{\text{EMB}}(\nu\omega_p) - \underline{U}_{D\nu}^{(k-1)} + \underline{U}_{S\nu} \right\}. \tag{21}$$

Note that (21) is equivalent to (10) and (11) when $Z_D(\nu\omega_p) \to \infty$ ($i = \text{const}$) and when $Z_D(\nu\omega_p) \to 0$ ($u = \text{const}$), respectively.

The remaining problem is to give an expression for the source impedance $Z_D(\nu\omega_p)$.

In the case of a small-signal problem, the source impedance of the diode at the kth iteration period is simply given by the small-signal conductance and capacitance of the previously calculated period

$$\underline{Z}_D^{(k)}(\nu\omega_p) = \frac{1}{G_0^{(k-1)} + j\nu\omega_p C_0^{(k-1)}} \tag{22}$$

where

$$G_0^{(k-1)} = \frac{1}{T}\int_0^T G_j(t)\,dt = \frac{I_s}{\eta U_T \cdot T}\int_0^T e^{u_D^{(k-1)}(t)/\eta \cdot U_T}\,dt \tag{23}$$

$$C_0^{(k-1)} = \frac{1}{T}\int_0^T C_j(t)\,dt = \frac{C_{j0}}{T}\int_0^T \left(1 - \frac{U_D^{(k-1)}(t)}{\psi}\right)^{\gamma} dt. \tag{24}$$

As G_0 and C_0 are the zeroth Fourier coefficients of $G_j(t)$ and $C_j(t)$, a FFT algorithm can be used to compute these coefficients.

It will be shown below by comparing the convergence of different numerical techniques, that this equation, derived from a small-signal analysis, can be used successfully even in the case of the large-signal analysis.

It is obvious, that the small-signal values of (23) and (24) are valid rigorously only for an operating point that remains constant. Hence, the most critical case is a strong change of the operating point during the iteration procedure. In this case, it is advantageous to determine the auxiliary source U_{a0} together with U_{a1} and U_{b1} first, and then to start determining all harmonic sources together. A strong change of the operating point implies that we are dealing with one of the limiting cases of (10) and (11); thus, the starting procedure for adjusting U_{a0} makes use of these equations.

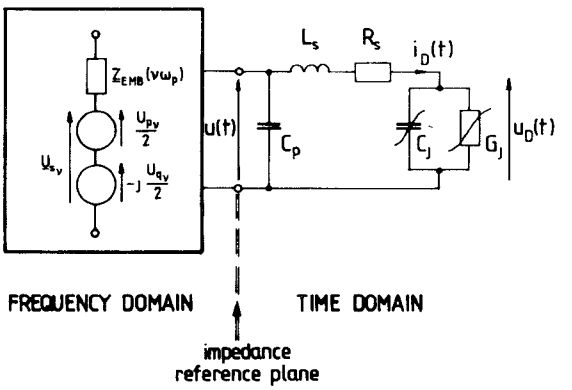

Fig. 3. Time-domain description, when the diode's parasitics are included in the nonlinear problem.

C. Refining the Numerical Technique

When formulating the nonlinear problem in the time domain, it is simplest to use the barrier of the diode instead of the diode's outer terminals as a junction plane between the time and frequency domains. The reason for this is the reduction of the order of the differential equation in the time domain. In this case, the parasitic elements of the diode, as shown in Fig. 3, are included in the embedding impedances of the frequency-domain description.

Considering all parasitic elements of the diode in the time-domain analysis, the order of the differential equation increases from 1 to 3, and an increase of calculation time can be assumed.

This might be the reason for the fact that all the authors who have dealt with a nonlinear mixer analysis incorporating harmonic balance techniques have included the diode's parasitics into the frequency-domain description. On the other hand, the signal at the diode's outer terminals is more band-limited due to the low-pass character of the parasitic circuitry. Hence, we expect a reduction of the aliasing error of the FFT when the parasitic elements are included in the time-domain part of the circuit, as shown in Fig. 3.

If $\underline{Z}_{\mathrm{GEN}}$ is chosen to be purely resistive, a system of differential equations is obtained as follows:

$$\frac{duu_D^{(k)}(t)}{dt} = \frac{\left(1-\dfrac{u_D^{(k)}(t)}{\psi}\right)^{\gamma}}{C_{j0}}\left\{i_D(t) - I_s\left(e^{u_D^{(k)}(t)/\eta U_T}-1\right)\right\} \tag{25}$$

$$\frac{di_D^{(k)}(t)}{dt} = \frac{1}{L_S}\left\{u^{(k)}(t) - u_D^{(k)}(t) - R_S \cdot i_D^{(k)}(t)\right\}. \tag{26}$$

$$\frac{du^{(k)}(t)}{dt} = \frac{1}{C_p}\left\{\left(u_S(t) + u_A^{(k-1)}(t) - u^{(k)}(t)\right)/R_{\mathrm{GEN}} - i_D^{(k)}(t)\right\} \tag{27}$$

where $u_S(t)$ is given by (8). The time-domain representation of the auxiliary source $u_A^{(k-1)}(t)$ is given by (9) with the frequency-domain descriptions according to (12), (13), and (21) and can be calculated as an inverse Fourier transform. In general, it is advantageous to reduce the bandwidth of the inverse Fourier transform through smoothing by means of a cubic spline interpolation; the increase of computing time is negligible.

In order to compare the computing time requirements of both of the time-domain formulations according to Figs. 1 and 3, the following situation will be considered. The diode is chosen to be a typical beam-lead Si Schottky-barrier diode for microwave applications

$$I_s = 0.5\ 10^{-7}\ \mathrm{A};\quad \eta = 1.08;\quad \gamma = 0.5;\quad \psi = 0.6\ \mathrm{V};$$
$$C_{j0} = 0.25\ \mathrm{pF};$$
$$C_p = 0.1\ \mathrm{pF};\quad L_S = 0.1\ \mathrm{nH};\quad R_S = 2.5\ \Omega;$$
$$U_T = 0.026\ \mathrm{V}.$$

The even-harmonic impedances are assumed to be

$$\underline{Z}_{\mathrm{EMB}}(2\nu\omega_p) = \frac{1}{\mu}\cdot 50\ \Omega, \qquad \mu = \begin{cases} 2 \\ 5 \end{cases} \tag{28}$$

and the odd-harmonic impedances are assumed to be

$$\underline{Z}_{\mathrm{EMB}}\left[(2\nu-1)\omega_p\right] = \mu \cdot 50\ \Omega, \qquad \mu = \begin{cases} 2 \\ 5 \end{cases} \tag{29}$$

and the source impedance has been chosen to be $\underline{Z}_{\mathrm{GEN}} = R_{\mathrm{GEN}} = 50\ \Omega$. It should be pointed out that the impedance

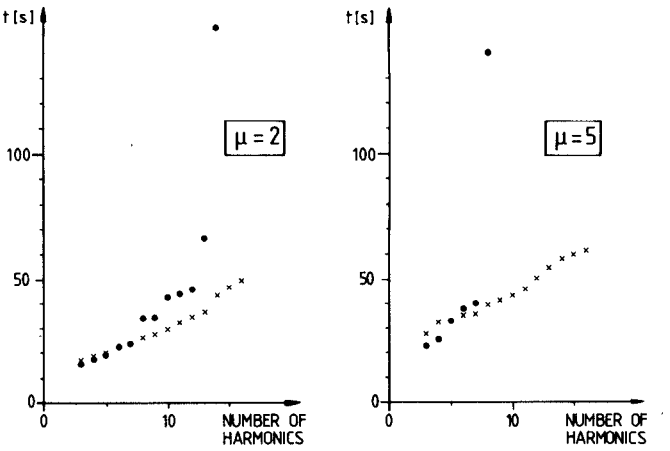

Fig. 4. Computing time requirements against the number of adjusted harmonics for an LO power range from 0 dBm to +10 dBm in steps of 1 dB. The embedding network is given by (28) and (29). ×: diode's parasitics in time-domain analysis. ∘: diode's parasitics in frequency-domain analysis.

situation according to $\mu = 2$ typically occurs in balanced mixer configurations at low frequencies.

Let us consider the LO power to be varied between 0 dBm and +10 dBm in steps of 1 dB, which is a typical LO drive range when dealing with silicon Schottky-barrier diodes of a medium barrier height. The pump frequency is chosen to be $f_p = 5$ GHz.

The adjustment of the harmonic impedances is truncated and the solution is accepted if the mean harmonic impedance error is

$$\bar{e} = \frac{1}{n+1}\sum_{\nu=0}^{n} e_\nu \leqslant 0.001 \tag{30}$$

where

$$e_\nu = \left|1 - \frac{\underline{U}_{S\nu} - \underline{U}_{D\nu}}{\underline{I}_{D\nu}\cdot \underline{Z}_{\mathrm{EMB}}(\nu\omega_p)}\right|. \tag{31}$$

In Fig. 4, the required computing time on a CYBER 170-835 is plotted against the number of harmonics being adjusted. If the diode's parasitics are included in the time-domain description (Fig. 3), the computing time increases slightly with increasing μ and an increasing number of harmonics being adjusted.

If the diode barrier is chosen to be the impedance reference plane (Fig. 1), a stronger increase of computing time is recognizable, leading to divergence in the cases

$$\mu = 2;\ \nu > 14 \quad \text{and} \quad \mu = 5;\ \nu > 7.$$

It should be pointed out that, when the diode parasitics are considered part of the frequency-domain circuit, the convergence decreases much more rapidly if the above-mentioned cubic sline interpolation is not applied, whereas its influence is only slight when the diode's parasitics are included in the time-domain analysis.

As a result, it has been demonstrated for two sets of embedding impedances that including the diode's parasitics in the time-domain analysis leads to a more efficient and reliable numerical technique than including them in the frequency-domain analysis, even though the order of the

differential equation set is increased. This is due to the fact that we deal with a more band-limited signal at the junction plane between the time and frequency domains when including the parasitics into the time-domain description.

The difference between the two formulations becomes more pronounced with increasing the number of harmonics and with increasing the complexity of the embedding network.

Finally, some comments will be made on the choice of $\underline{Z}_{GEN}$. As mentioned above, the choice of $\underline{Z}_{GEN}$ is arbitrary if auxiliary sources are established for all harmonics, including the average and first harmonics. If $\underline{Z}_{GEN}$ is chosen to be the lumped-element representation of the impedance at the first harmonic, then the auxiliary sources U_{a1} and U_{b1} are dispensable. In case of a positive reactance of $\underline{Z}_{EMB}(\omega_p)$, the lumped-element representation has to be chosen as a series connection of L_{GEN} and R_{GEN}, and in case of a negative reactance of $\underline{Z}_{EMB}(\omega_p)$, the lumped-element representation has to be chosen as a parallel connection of G_{GEN} and C_{GEN}. For these two cases, the time-domain differential equation sets are different.

It will be shown in Section III that the increased computational complexity yields an increased convergence rate. Hence, the choice of $\underline{Z}_{GEN}$ as the lumped-element representation of the embedding network at the fundamental is a useful initial guess for solving the nonlinear problem.

In case of a nonconvergent solution, it might be advantageous to make use of this degree of freedom by choosing a value of $\underline{Z}_{GEN}$ which leads to convergence.

A flow chart of the numerical nonlinear analysis is given in Fig. 5.

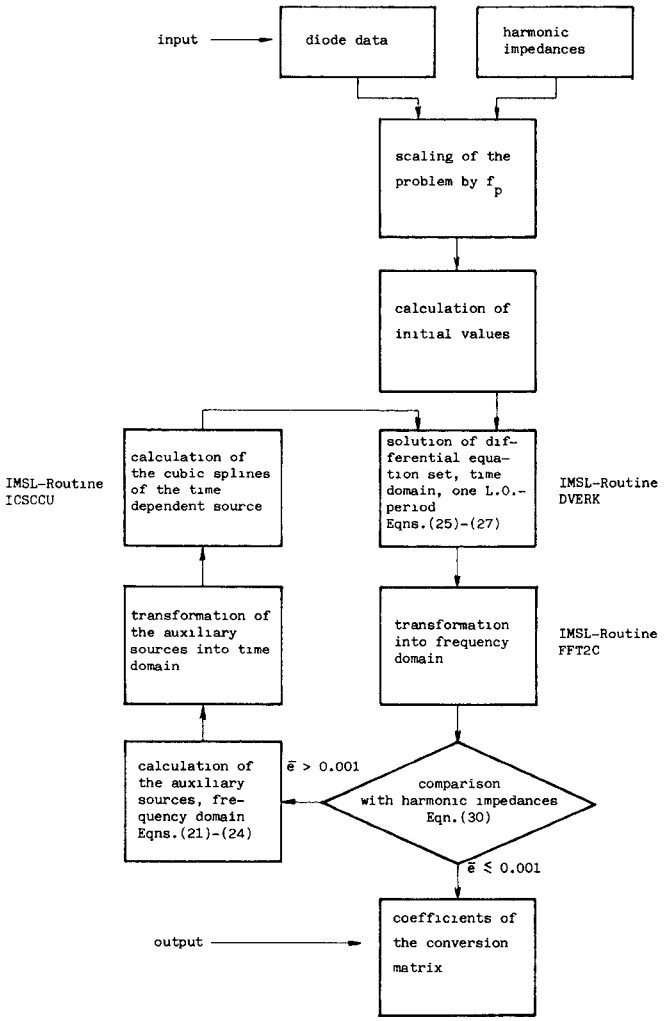

Fig. 5. Flow chart of the applied numerical technique.

III. Convergence Considerations

This section is intended to provide a comparison of the reliability and speed of different numerical techniques for solving the nonlinear problem.

First, a comparison is given using Kerr's data [6], which have also been used in [8] and [12]. Particular attention is given to the influence of the LO drive level. Then a more general comparison is made between the different techniques using harmonic impedance sets created by a random generator.

A. Convergence Comparison Using Kerr's Data

Kerr [6] has defined a convergence condition

$$C_\nu = \frac{\underline{U}_{S\nu} - \underline{U}_{D\nu}}{\underline{I}_{D\nu} \cdot \underline{Z}_{EMB}(\nu\omega_p)} \tag{32}$$

which must be equal to unity for a converged solution for all ν. Using (32), a convergence diagram has been obtained for his technique, showing the convergence condition as a function of the harmonic number after 100 iterations and 300 iterations, respectively (see Fig. 6(a)). Hicks and Khan [8] took up this diagram in order to compare their voltage update method with Kerr's method (Fig. 6(b)). Although the convergence is improved slightly by using a convergence parameter p, the computation time is of the same order of magnitude as Kerr's method. However, the optimum convergence parameter ($p = 0.025$ in this case) is not given by an analytical expression but has to be found by some trials, which is not satisfying when analyzing an unknown nonlinear circuit.

In order to give a comparison with the method presented in this paper, Fig. 6(c) shows the convergence conditions after 10 and 15 iterations, according to the numerical technique of Section II. A rather similar diagram has been obtained when the junction capacitance is allowed to vary with the junction voltage (Fig. 6(d)), which is the most realistic but critical case when dealing with microwave mixers incorporating Schottky-barrier diodes.

Assuming convergence if the convergence condition

$$1 - C_\nu \leq 0.5\%, \qquad \nu = 0 \cdots 16 \tag{33}$$

is fulfilled, Kerr's method requires about 500 iteration periods compared with 350 iteration periods of the Hicks and Khan approach. The technique presented here requires 20 iterations in the case of $C_j = \text{const}$ and 22 iterations if C_j is varying with the junction voltage.

It is noticeable that convergence is improved by a factor of ten or more even in the case of a voltage-dependent

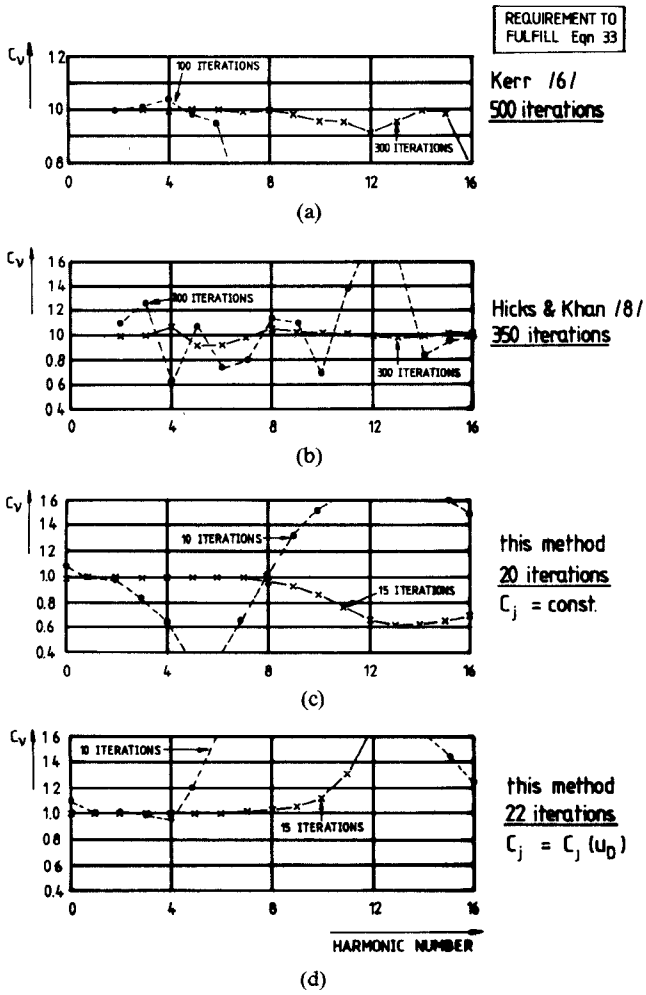

Fig. 6. Convergence diagrams using Kerr's data [6]. (a) Kerr [6]; 100 and 300 iteration periods. (b) Hicks and Khan [8]; 200 and 300 iteration periods. (c) This method; C_j = const, 10 and 15 iteration periods. (d) This method; $C_j = C_j(u_D)$; 10 and 15 iteration periods.

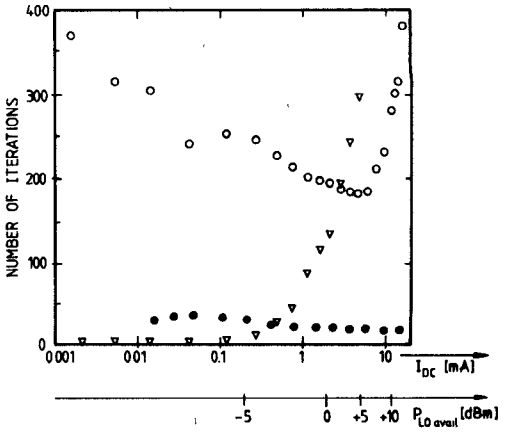

Fig. 7. Number of iterations required for solving Kerr's waveguide diode mixer (16 harmonics) against dc diode current and available LO power. ○: Hicks–Khan [8] (after [12]). ▽: Camacho-Peñalosa [12]. ●: This method.

junction capacitance. The results of Fig. 6 ignore the important influence of the LO drive level on the convergence rate. In Fig. 7, which is taken from [12], the number of iterations is plotted against the dc diode current, which is an inherent function of the LO drive level. If we assume the bias voltage is adjusted to give an angle of current flow $\theta = 90°$, then the available LO power is approximately given by the additionally noted abscissa values in Fig. 7. It should be noted that the angle of current flow does not differ so much from the assumed value of $\theta = 90°$, especially in the LO power range of interest. Hence, the additionally noted abscissa values give a good approximation of the available LO power which is necessary to achieve the dc current values given in Fig. 7. It can be seen that the methods described in [8] and [12] show a strongly decreased convergence rate in the LO drive range of interest (> 0 dBm), whereas the proposed method offers a convergence rate which is nearly independent of the LO drive. However, it should be mentioned that the convergence behavior in general depends on the embedding circuitry as well as on the LO power. A more general consideration of this problem is given in Section III-B.

B. Convergence Comparison Using Randomly Generated Impedance Data

Due to the fact that practical mixer circuits have a wide range of harmonic embedding impedances, a more general convergence comparison will be given here. Let

$$0 < \{\text{rand}\,1, \text{rand}\,2\} < 1 \tag{34}$$

be two independent random numbers. Then we can define a reflection coefficient

$$\underline{r} = |\text{rand}\,1| e^{j2\pi \cdot \text{rand}\,2}. \tag{35}$$

If a mixer shall be applied in a 50-Ω system, we can assume that every complex reflection coefficient of a 50-Ω system has the same probability, and we can define a corresponding set of random impedances

$$\underline{Z} = 50 \frac{1+\underline{r}}{1-\underline{r}} [\Omega]. \tag{36}$$

Let us restrict the number of harmonics to be within

$$0 \leqslant \nu \leqslant 4 \tag{37}$$

which is sufficiently high for the analysis of a real microwave mixer. Now we can calculate any number of harmonic impedances and take them for a convergence test. For a particular initiation of both of the random generators, 430 sets of harmonic impedance values have been obtained, as shown in Fig. 8, yielding 2150 different impedance values according to (37).

All the following considerations assume the LO voltage source to be a constant value of $u_p = 2$ V according to an available LO power of +10 dBm if the source impedance would be $\underline{Z}_{\text{EMB}}(\omega_p) = 50$ Ω. But as the source impedance at the first harmonic $\underline{Z}_{\text{EMB}}(\omega_p)$ is also randomly generated, in fact a wide LO drive range is applied to the diode.

Convergence is assumed if the mean impedance error of the harmonics $\nu = 0 \cdots 4$ given by (30) is $e \leqslant 0.005$.

Three different numerical techniques will be treated here in order to compare their rate of convergence.

The first technique is the voltage update method proposed by Hicks and Khan [8]. The lack of an analytical

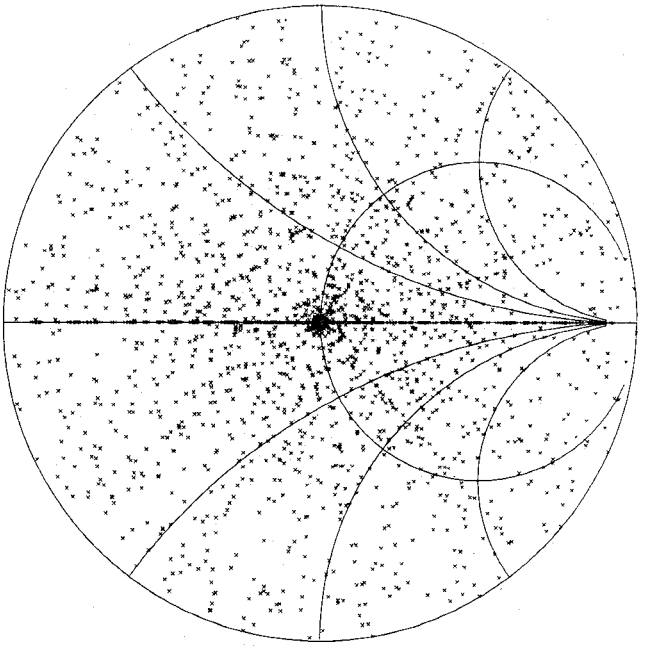

Fig. 8. 430 sets of randomly generated harmonic impedances.

expression for determining the convergence parameter p requires excessive computer time if a wide range of p is taken into consideration. In practice, p is varied between

$$0.02 \leqslant p \leqslant 1 \tag{38}$$

for each harmonic impedance set. If the required number of iterations is taken only for the optimum value of p (found by trial), we get a histogram of iteration periods as given in Fig. 9(a).

The second method under consideration is that proposed by Gwarek [7], which has been described briefly in Section II. Using his equations for determining the auxiliary sources (eqs. (10) and (11)), a histogram of iteration periods is obtained as given in Fig. 9(b).

Although the rate of convergence is poor (about 60 percent), the mean value of required iteration periods is decreased compared with Hicks' and Khan's method. But it is important to remember that no trials have to be made in order to find an optimum convergence parameter.

The third method which shall be considered here in depth is that proposed in this paper. Particular attention will be paid to the choice of the source impedance $\underline{Z}_{GEN}$ as mentioned in Section II-C.

If we choose $\underline{Z}_{GEN}$ to be the lumped-element representation of $\underline{Z}_{EMB}(\omega_p)$, a histogram is obtained as given in Fig. 9(c). In the case of choosing a purely resistive $\underline{Z}_{GEN} = 50\ \Omega$, we get the histogram of Fig. 9(d). Comparing both of these histograms, it can be seen that choosing $\underline{Z}_{GEN}$ to be the lumped-element representation of the embedding network at the fundamental yields a significantly increased convergence rate.

Remembering the fact that we have an additional degree of freedom in choosing $\underline{Z}_{GEN}$ when analyzing an unknown nonlinear circuit, the question arises whether its choice can lead to an increased convergence rate in general. The

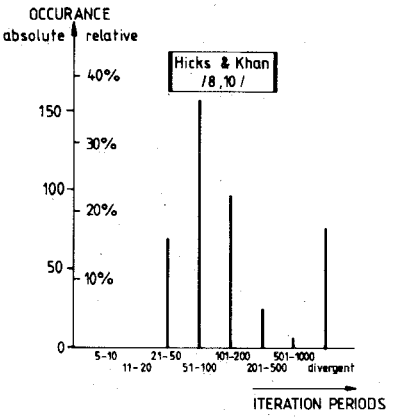

(a)

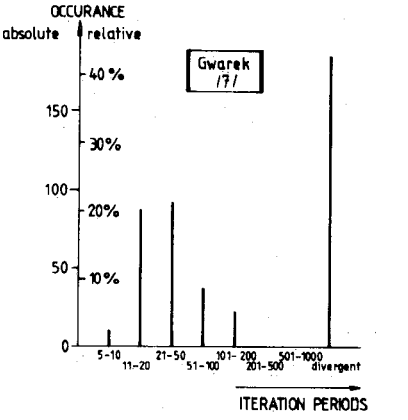

(b)

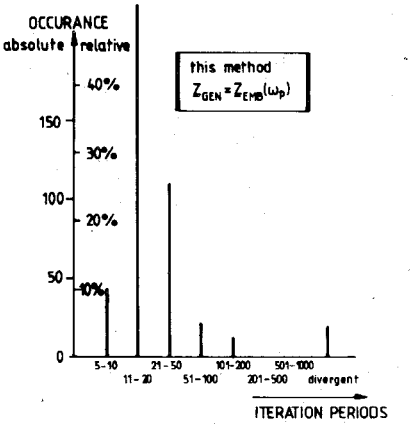

(c)

Fig. 9. Histograms of required iteration periods. (a) Hicks and Khan [8], various convergence parameters, optimum determined by trial. (b) Gwarek [7]. (c) This method, $\underline{Z}_{GEN} = \underline{Z}_{EMB}(\omega_p)$ (lumped-element representation of the embedding network at the fundamental).

histogram of Fig. 9(e) is obtained if we use both source impedance cases alternatively and choose the fastest. Convergence now occurs in 99 percent of cases.

Comparing the histograms of Fig. 9(c) (this method) and Fig. 9(a) (Hicks and Khan), we have to remember that Fig. 9(a) is obtained by varying the convergence parameter in a wide range and choosing the optimum value for each harmonic impedance set. In other words, the presented histogram of Fig. 9(a) would be obtained without trial if an

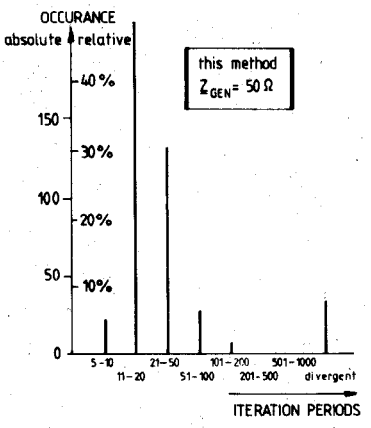

(d)

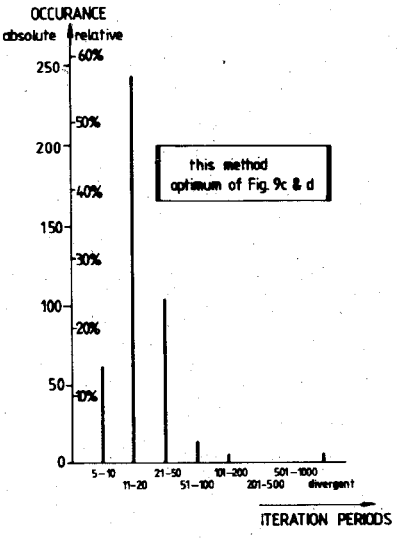

(e)

Fig. 9 (*cont.*) (d) This method, purely resistive $\underline{Z}_{GEN} = 50\ \Omega$. (e) Using the fastest of (c) and (d).

analytic expression for the convergence parameter would be available. Hence, the histogram of Fig. 9(a) has to be interpreted as an optimistic presentation of the convergence behavior of this method.

Comparing the histograms of Fig. 9(c) (this method) and Fig. 9(b) (Gwarek), it has been demonstrated that including an effective diode impedance at each harmonic when determining the auxiliary sources (16)–(24) leads to a significantly improved convergence in general.

The results of this chapter are summarized in Table I, where the percentage of divergence as well as the mean value of required iteration periods is given for the methods under consideration.

In conclusion, it should be pointed out that the proposed numerical technique is very efficient and reliable. If a larger number of harmonics is taken into account, the advantage of this method is much greater. This is because the magnitude of higher harmonics generated by the diode decreases and, hence, the small-signal conditions of (23) and (24) are increasingly fulfilled with an increasing number of harmonics.

TABLE I

method	histogram	divergent	mean value of required iteration periods
Hicks–Khan	Fig. 9(a)	17%	99.1
Gwarek	Fig. 9(b)	43%	39.6
This Method			
$\underline{Z}_{GEN} = Z_{EMB}(\omega_p)$	Fig. 9(c)	5%	24.7
$\underline{Z}_{GEN} = 50\ \Omega$	Fig. 9(d)	10%	23.9
Choosing the fastest of 9(c) and 9(d)	Fig. 9(e)	1%	19.1

IV. Linear Analysis

Having determined the voltage waveform at the diode's barrier, the instantaneous values of the differential conductance and capacitance can be calculated by (2) and (3) leading to their Fourier transforms through

$$G_\mu = \frac{1}{T}\int_0^T G_j(t)\, e^{-j\mu\omega_p t}\, dt \tag{39}$$

$$C_\mu = \frac{1}{T}\int_0^T C_j(t)\, e^{-j\mu\omega_p t}\, dt. \tag{40}$$

When formulating the linearized problem by means of an admittance matrix

$$\begin{matrix}\text{sum}\rightarrow\\ \text{signal}\rightarrow\\ \text{IF}\rightarrow\\ \text{image}\rightarrow\end{matrix}\begin{pmatrix}\vdots\\ \underline{I}_2\\ \underline{I}_1\\ \underline{I}_0\\ \underline{I}_{-1}\\ \underline{I}_{-2}\\ \vdots\end{pmatrix} = \begin{pmatrix} & \vdots & \vdots & \vdots & \vdots & \vdots & \\ \cdots & Y_0 & \underline{Y}_1 & \underline{Y}_2 & \underline{Y}_3 & \underline{Y}_4 & \cdots \\ \cdots & \underline{Y}_1^* & Y_0 & \underline{Y}_1 & \underline{Y}_2 & \underline{Y}_3 & \cdots \\ \cdots & \underline{Y}_2^* & \underline{Y}_1^* & Y_0 & \underline{Y}_1 & \underline{Y}_2 & \cdots \\ \cdots & \underline{Y}_3^* & \underline{Y}_2^* & \underline{Y}_1^* & Y_0 & \underline{Y}_1 & \cdots \\ \cdots & \underline{Y}_4^* & \underline{Y}_3^* & \underline{Y}_2^* & \underline{Y}_1^* & Y_0 & \cdots \\ & \vdots & \vdots & \vdots & \vdots & \vdots & \end{pmatrix} \cdot \begin{pmatrix}\vdots\\ \underline{U}_2\\ \underline{U}_1\\ \underline{U}_0\\ \underline{U}_{-1}\\ \underline{U}_{-2}\\ \vdots\end{pmatrix} \tag{41}$$

which can be expressed as

$$\underline{I}_m = \sum_{\mu=-\infty}^{+\infty} \underline{Y}_{m-\mu}\cdot\underline{U}_\mu \tag{42}$$

where the according frequencies are

$$f_m = |m\cdot f_p + f_{IF}|. \tag{43}$$

The coefficients of this conversion matrix can be calculated from the Fourier transforms of G_j and C_j as follows:

$$\underline{Y}_{m-\mu} = \mathrm{Re}\{\underline{G}_{m-\mu}\} - (m\omega_p + \omega_0)\,\mathrm{Im}\{\underline{C}_{m-\mu}\} + j\left[\mathrm{Im}\{\underline{G}_{m-\mu}\} + (m\omega_p + \omega_0)\,\mathrm{Re}\{\underline{C}_{m-\mu}\}\right]. \tag{44}$$

If we choose a description of the linearized problem through an $m\times m$ matrix, this matrix can be reduced to a 2×2 matrix if the impedance relations at $m-2$ mixing products are given by

$$\underline{I}_m = -\underline{Y}_{(m)}\cdot u_m \tag{45}$$

where $Y_{(m)}$ represents the load admittance at the mth mixing product (see Fig. 10). Then the power flow between any of the mixing products can be calculated for a fundamental or subharmonically pumped mixer. The only difference between these two cases is the succession of the matrix reduction, arranged by an exchange of rows and columns of the conversion matrix. Depending on the

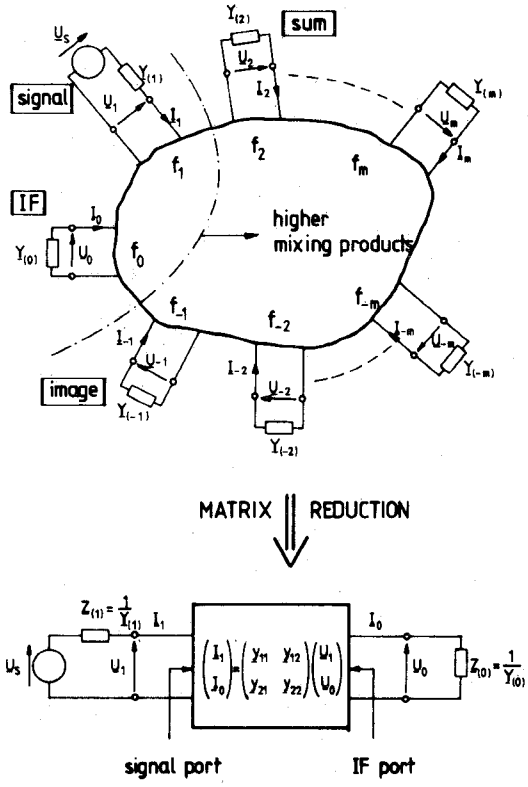

Fig. 10. Linearized problem: reduction of the frequency multiport to a 2-port.

matching conditions at the input and/or output port, different conversion losses can be defined.

If no matching takes place, the transducer conversion loss can be calculated, given by

$$L_c = \frac{\text{power available from signal source}}{\text{power delivered to IF load}}$$

$$L_c = \frac{\left|\left(\underline{y}_{11}+\underline{Y}_{(1)}\right)\left(\underline{y}_{22}+Y_{(2)}\right)-\underline{y}_{12}\cdot\underline{y}_{21}\right|^2}{4\cdot\mathrm{Re}\left\{\underline{Y}_{(1)}\right\}\cdot\mathrm{Re}\left\{\underline{Y}_{(2)}\right\}\cdot\left|\underline{y}_{21}\right|^2} \tag{46}$$

where the $\underline{y}_{ij}$ represent the coefficients of the reduced 2×2 conversion matrix, $Y_{(1)}$ is the signal source impedance, and $Y_{(0)}$ is the IF load impedance (see Fig. 10).

Other conversion losses can simply be calculated from the coefficients of the 2×2 conversion matrix but will not be considered here.

V. Particularities of Balanced Mixer Analysis

In the analysis of a balanced mixer, it is advantageous to make use of its symmetry properties if we assume the diodes to be identical. The influence on the nonlinear and linear mixer analysis will be regarded separately. It will be shown that a balanced mixer can be treated as a single diode mixer as previously considered in [4]. In the nonlinear analysis, the impedance conditions given by the embedding network have to be rearranged. The linearized problem can be solved by a simple change of the coefficients of the conversion matrix.

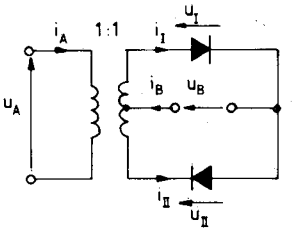

Fig. 11. Basic equivalent circuit of a balanced mixer, considering the nonlinear problem.

A. Nonlinear Analysis of Balanced Mixers

Let us consider an equivalent circuit of a balanced mixer as sketched in Fig. 11. Due to the opposite polarity of the diodes, we have

$$i_{\mathrm{II}}(\omega_p t) = -\,i_{\mathrm{I}}(\omega_p t+\pi). \tag{47}$$

Expressing i_A and i_B in terms of Fourier series yields

$$i_A(\omega_p t) = \frac{1}{2}\sum_{\nu=-\infty}^{+\infty}\underline{I}_{\mathrm{I}2\nu}e^{j2\nu\omega_p t} \tag{48}$$

$$i_B(\omega_p t) = \frac{1}{2}\sum_{\nu=-\infty}^{+\infty}2\underline{I}_{\mathrm{I}(2\nu-1)}e^{j(2\nu-1)\omega_p t} \tag{49}$$

where i_A and i_B are formulated only to be a function of the current through diode I.

Expressing u_A and u_B in terms of Fourier series yields

$$u_A(\omega_p t) = \frac{1}{2}\sum_{\nu=-\infty}^{+\infty}2\underline{U}_{\mathrm{I}2\nu}e^{j2\nu\omega_p t} \tag{50}$$

$$u_B(\omega_p t) = \frac{1}{2}\sum_{\nu=-\infty}^{+\infty}\underline{U}_{\mathrm{I}(2\nu-1)}e^{j(2\nu-1)\omega_p t}. \tag{51}$$

Calculating the impedances seen by only one diode, we get in case of the odd harmonics

$$\frac{\underline{U}_{\mathrm{I}(2\nu-1)}}{\underline{I}_{\mathrm{I}(2\nu-1)}} = 2\frac{\underline{U}_{B(2\nu-1)}}{\underline{I}_{B(2\nu-1)}} = 2\underline{Z}_{\mathrm{EMB}}\left[(2\nu-1)\omega_p\right] \tag{52}$$

and in case of the even harmonics

$$\frac{\underline{U}_{\mathrm{I}2\nu}}{\underline{I}_{\mathrm{I}2\nu}} = \frac{1}{2}\frac{\underline{U}_{A2\nu}}{\underline{I}_{A2\nu}} = \frac{1}{2}\underline{Z}_{\mathrm{EMB}}(2\nu\omega_p) \tag{53}$$

so we can approach the nonlinear problem by considering only one diode, with embedding impedances at the diode plane given by (52) and (53). Note that these impedances are at a virtual impedance reference plane and do not exist physically.

B. Linear Analysis of Balanced Mixers

The basic circuitry of Fig. 11 has to be rearranged for the small-signal case considered in this section. Both the diodes are to be replaced by their time-varying admittances as shown in Fig. 12. The time-varying admittances do contain the solution of the nonlinear problem as given by the diode's nonlinearities and the harmonic impedances.

It can easily be verified that the mixing products are split up in such a way that the even mixing products $m=2n$ appear at port B, whereas port A only contains

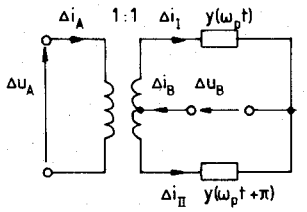

Fig. 12. Basic equivalent circuit of a balanced mixer, considering the linearized problem.

odd mixing products ($m = 2n - 1$). Due to the voltage splitting at port A and the current splitting at port B, (41) can be written as

$$\begin{pmatrix} \vdots \\ \frac{1}{2}\underline{I}_2 \\ \underline{I}_1 \\ \frac{1}{2}\underline{I}_0 \\ \underline{I}_{-1} \\ \frac{1}{2}\underline{I}_{-2} \\ \vdots \end{pmatrix} = \begin{pmatrix} \cdots & \vdots & \vdots & \vdots & \vdots & \vdots & \\ \cdots & Y_0 & \underline{Y}_1 & \underline{Y}_2 & \underline{Y}_3 & \underline{Y}_4 & \cdots \\ \cdots & \underline{Y}_1^* & Y_0 & \underline{Y}_1 & \underline{Y}_2 & \underline{Y}_3 & \cdots \\ \cdots & \underline{Y}_2^* & \underline{Y}_1^* & Y_0 & \underline{Y}_1 & \underline{Y}_2 & \cdots \\ \cdots & \underline{Y}_3^* & \underline{Y}_2^* & \underline{Y}_1^* & Y_0 & \underline{Y}_1 & \cdots \\ \cdots & \underline{Y}_4^* & \underline{Y}_3^* & \underline{Y}_2^* & \underline{Y}_1^* & Y_0 & \cdots \\ & \vdots & \vdots & \vdots & \vdots & \vdots & \end{pmatrix} \cdot \begin{pmatrix} \vdots \\ \underline{U}_2 \\ \frac{1}{2}\underline{U}_1 \\ \underline{U}_0 \\ \frac{1}{2}\underline{U}_{-1} \\ \underline{U}_{-2} \\ \vdots \end{pmatrix}$$

current splitting at port B; voltage splitting at port A (54)

Including the factors 1/2 into the conversion matrix yields

$$\begin{matrix} \\ \text{port B} \\ \text{port A} \\ \text{port B} \\ \text{port A} \\ \text{port B} \end{matrix} \begin{pmatrix} \vdots \\ \underline{I}_2 \\ \underline{I}_1 \\ \underline{I}_0 \\ \underline{I}_{-1} \\ \underline{I}_{-2} \\ \vdots \end{pmatrix} = \begin{pmatrix} \cdots & \vdots & \vdots & \vdots & \vdots & \vdots & \\ \cdots & 2Y_0 & \underline{Y}_1 & 2\underline{Y}_2 & \underline{Y}_3 & 2\underline{Y}_4 & \cdots \\ \cdots & \underline{Y}_1^* & \frac{Y_0}{2} & \underline{Y}_1 & \frac{\underline{Y}_2}{2} & \underline{Y}_3 & \cdots \\ \cdots & 2\underline{Y}_2^* & \underline{Y}_1^* & 2Y_0 & \underline{Y}_1 & 2\underline{Y}_2 & \cdots \\ \cdots & \underline{Y}_3^* & \frac{\underline{Y}_2^*}{2} & \underline{Y}_1^* & \frac{\underline{Y}_0}{2} & \underline{Y}_1 & \cdots \\ \cdots & 2\underline{Y}_4^* & \underline{Y}_3^* & 2\underline{Y}_2^* & \underline{Y}_1^* & 2Y_0 & \cdots \\ & \vdots & \vdots & \vdots & \vdots & \vdots & \end{pmatrix} \cdot \begin{pmatrix} \vdots \\ \underline{U}_2 \\ \underline{U}_1 \\ \underline{U}_0 \\ \underline{U}_{-1} \\ \underline{U}_{-2} \\ \vdots \end{pmatrix} \quad (55)$$

This final formulation is valid at both of the mixer ports (A and B) where the conversion matrix is given by the Fourier coefficients of a single diode, but describing the frequency conversion of a balanced mixer.

VI. Conclusion

An improved method of analysis of microwave mixers has been presented, which includes an efficient and reliable numerical technique for solving the nonlinear pumping problem. Single-ended and balanced mixers are considered. The efficiency and reliability of convergence has been demonstrated by comparing the proposed method with those which have been published previously.

Acknowledgment

The author wishes to acknowledge gratefully Prof. John for useful discussions and encouragement during the course of the research project.

References

[1] H. C. Torrey and C. A. Whitmer, *Crystal Rectifiers* (MIT Radiation Lab. Series, vol. 15). New York: McGraw-Hill, 1948.
[2] P. H. Siegel and A. R. Kerr, The measured and computed performance of a 140–200-GHz Schottky diode mixer," *IEEE Trans. Microwave Theory Tech.*, vol. MTT-32, pp. 1579–1590, 1984.
[3] D. N. Held and A. R. Kerr, "Conversion loss and noise of microwave and millimeter-wave mixers. Parts 1+2," *IEEE Trans. Microwave Theory Tech.*, vol. MTT-26, pp. 49–61, 1978.
[4] A. R. Kerr, "Noise and loss in balanced and subharmonically-pumped mixers: Part 1—Theory, Part 2—Application," *IEEE Trans. Microwave Theory Tech.*, vol. MTT-27, pp. 938–950, 1979.
[5] R. G. Hicks and P. J. Khan, "Numerical analysis of subharmonic mixers using accurate and approximate models," *IEEE Trans. Microwave Theory Tech.*, vol. MTT-30, pp. 2113–2120, 1982.
[6] A. R. Kerr, "A technique for determining the local oscillator waveforms in a microwave mixer," *IEEE Trans. Microwave Theory Tech.*, vol. MTT-23, pp. 828–831, 1975.
[7] W. K. Gwarek, "Nonlinear analysis of microwave mixers," M. S. thesis, MIT, Cambridge, MA, Sept. 1974.
[8] R. G. Hicks and P. J. Khan, "Numerical technique for determining pumped nonlinear device waveforms," *Electron. Lett.*, vol. 16, pp. 375–376, 1980.
[9] S. Egami, Nonlinear, linear analysis and computer aided design of resistive mixers," *IEEE Trans. Microwave Theory Tech.*, vol. MTT-22, pp. 270–275, 1974.
[10] R. G. Hicks and P. J. Khan, "Numerical analysis of nonlinear solid-state device excitation in microwave circuits," *IEEE Trans. Microwave Theory Tech.*, vol. MTT-30, pp. 251–259, 1982.
[11] B. Schüppert, "Modified numerical method for solving the nonlinear mixer pumping problem," *Electron. Lett.*, vol. 19, pp. 50–52, 1983.
[12] C. Camacho-Peñalosa, "Numerical steady-state analysis of nonlinear microwave circuits with periodic excitation," *IEEE Trans. Microwave Theory Tech.*, vol. MTT-31 pp. 724–730, 1983.
[13] B. Schüppert, "Analysis and design of microwave balanced mixers," this issue, pp. 120–128.

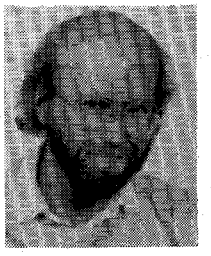

Bernd Schüppert was born June 5, 1947, in Neunkirchen, West Germany. He received the Dipl.-Ing. degree (1978) and the Dr.-Ing. degree (1983), both in electrical engineering, from the Technische Universität Berlin.

Since 1978, he has been a Research Associate at the Technische Universität Berlin, Institut für Hochfrequenztechnik, working on mixer problems, both theoretically and experimentally. During 1983–1984, he worked on a research project on planar balanced broad-band mixers, sponsored by the Deutsche Forschungsgemeinschaft. Since 1983, he has been working on Ti: $LiNbO_3$ integrated optic devices as a head of the technology group at the Institute für Hochfrequenztechnik.

Dr. Schüppert is a member of the VDE/NTG (Germany).